PCCP

Diffusion of adsorbates on single crystal surfaces of square symmetry: finite-size scaling and the thermodynamic limit

F. Nieto,[a] A. A. Tarasenko[bc] and C. Uebing[d]

[a] *Departamento de Física and Centro Latinoamericano de Estudios Ilya Prigogine, Universidad Nacional de San Luis, CONICET, Chacabuco 917, 5700 San Luis, Argentina*
[b] *Institute of Physics, National Academy of Sciences of Ukraine, prospekt Nauki 46, 252028 Kyiv 28, Ukraine*
[c] *Institute of Physics, Academy of Sciences of the Czech Republic, Na Slovance 2, 182 21 Prague 8, Czech Republic*
[d] *Department of Physics and Astronomy, Rutgers University, 136 Frelinghuysen Rd., Piscataway NJ, 08854-8019, USA*

Received 14th November 2001, Accepted 17th January 2002
First published as an Advance Article on the web 4th April 2002

We investigate the influence of different diffusion mechanisms on the finite-size scaling behavior of the tracer surface diffusion coefficient in the close vicinity of a second order phase transition. A given diffusion mechanism emerges from a specific transition algorithm (TA) representing a microscopic model of adatom jumps on the surface. In this work we apply the Monte Carlo method to investigate a lattice gas model of repulsively interacting particles on a square lattice. For all diffusion mechanisms and lattice sizes L studied, the measured tracer surface diffusion coefficient, D_t, is a smooth function of temperature and exhibits an inflexion point at or near the critical temperature. Its derivative, $\partial D_t/\partial(1/k_B T)$, exhibits cusp-like maxima which are (a) sharply pronounced and (b) converge to $T_c(L=\infty)$ for large lattice sizes. We have analysed the finite-size behavior of D_t and obtained its critical exponent, σ_t, for each diffusion mechanism considered. The results show that σ_t is different for the different diffusion mechanism, *i.e.* σ_t depends on the choice of the TA.

1 Introduction

Surface diffusion of adsorbates on metal and alloy surfaces has become an important subject of surface science. The detailed comprehension of surface diffusion is one of the key steps in understanding (and controlling) many interesting surface phenomena such as adsorption, desorption, catalytic reactions, melting, roughening, and crystal and film growth. Despite the widespread availability of experimental techniques for the measurement of surface diffusion coefficients, a lot more work remains to be done for a complete understanding of this phenomenon. In many cases the interpretation of experimental surface diffusion data has been rather tedious, especially in heterogeneous systems and systems undergoing phase transitions. Therefore, many different theoretical and numerical methods such as mean-field,[1–4] Bethe–Peierls,[5] real-space renormalization group (RSRG),[6–8] transfer matrix[9] and Monte Carlo (MC)[10–14] methods have been used in order to describe the surface diffusion phenomenon.

The MC technique is probably one of the most reliable methods which can be used to study static and dynamic properties of adsorbed monolayers on metal surfaces by means of lattice gas modeling. The widespread availability of powerful computers and the simplicity to code MC computer algorithms have led to the success of this method. MC studies of adatom diffusion on different lattices and for various sets of the interaction parameters have been performed during the last two decades. Many of the earlier Monte Carlo studies of adsorbate diffusion have been reviewed by Kehr and Binder.[15] Lattice gas models have led to important conclusions about modern theories of phase transitions[16–20] and critical phenomena.[21,22] Static physical quantities like total energy, susceptibility *etc.* are subject to finite-size scaling effects close to a critical point.

2 Basics of surface diffusion

In this section we attempt to provide the basic background needed to understand both the computational procedures and the simulation results, which will be described in the following parts of this contribution.

The surface tracer diffusion coefficient

The surface tracer diffusion coefficient, D_t, describes the random walk of a tagged single particle. It is probably important to note that also the notation D^* is used for this quantity. D_t is defined through the generalized definition

$$D_t = \lim_{t\to\infty}\left[\frac{1}{2dt}\left\langle|\vec{r}_i(t)-\vec{r}_i(0)|^2\right\rangle\right] \quad (1)$$

where d is the Euclidean dimension, (in the case of surface diffusion $d=2$); the vector $\vec{r}(t)$ determines the position of a tagged particle at time t, and $\langle(\vec{r}(t)-\vec{r}(0))^2\rangle$ is its mean square displacement. Assuming that the particle executes jumps in either the $\pm x$, $\pm y$ or $\pm z$ directions, we can write

$$\left\langle(\vec{r}(t)-\vec{r}(0))^2\right\rangle = \langle(\Delta r)\rangle^2 = a_x^2 N_x(t) + a_y^2 N_y(t) + a_z^2 N_z(t). \quad (2)$$

Here $a_{x,y,z}$ denote the jump lengths for the corresponding directions, and $N_{x,y,z}(t)$ denote the corresponding number of

 DOI: 10.1039/b110413f

jumps taken in time t. For a square surface eqn. (1) can be rewritten as

$$D_t = \lim_{t\to\infty} \frac{1}{4t} \left\langle (\Delta r)^2 \right\rangle = \lim_{t\to\infty} \frac{1}{4t} \left[a_x^2 N_x(t) + a_y^2 N_y(t) \right] = \lim_{t\to\infty} \frac{1}{4t} a^2 N_{tot}(t), \quad (3)$$

if $a_x = a_y$ and $N_{tot} = N_x + N_y$. The quantity N_{tot}/t can be considered as an effective jump frequency[23]

$$\lim_{t\to\infty} \frac{N_{tot}}{t} = \nu_{eff} = \nu \exp\left(-\frac{E_d}{k_B T} \right) \quad (4)$$

with E_d as effective activation energy for adatom jumps. Thus D_t can be written as

$$D_t = \frac{1}{4} a^2 \nu \exp\left(-\frac{E_d}{k_B T} \right). \quad (5)$$

2.2 Simulations of surface diffusion

For the computer simulation of surface diffusion two powerful methods are frequently used, the molecular dynamics (MD) scheme (see *e.g.* refs. 15, 19, 20 and 24–26) and the Monte Carlo (MC) scheme. Since the study to be discussed in Section 5 is based on a lattice gas model investigated *via* MC simulations, we will discuss this method in some detail here.

Within the lattice gas scheme the basic steps of surface diffusion are jumps of adatoms from filled initial sites i to adjacent vacant sites f. The activation energy for such jumps can be calculated as the energy difference between saddle point $\varepsilon^*_{i\to f}$ and single site energy of the initial site ε_i,[14]

$$\Delta E = \varepsilon^*_{i\to f} - \varepsilon_i. \quad (6)$$

The associated jump probability P_J is given by

$$P_J = \frac{1}{\kappa} \exp\left(-\frac{\Delta E}{k_B T} \right), \quad (7)$$

with κ as a normalization factor. This choice ensures full microscopic reversibility and fulfils the condition of detailed balance.[27] However, the activation energies ΔE and the jump probabilities P_J are partly arbitrary since the detailed balance condition does not specify these quantities uniquely.[15] In order to optimize the computational time of a Monte Carlo algorithm, a suitable normalization of jump probabilities is indispensable. A natural choice for κ would be

$$\kappa = \kappa_{max} = \exp\left(-\frac{\Delta E_{min}}{k_B T} \right). \quad (8)$$

Here ΔE_{min} represents the jump probability for the most favorable physically realizable jump.[14] This choice of κ generates the highest possible jump probabilities, *i.e.*, minimizes the number of unsuccessful attempts, while avoiding jump events with $P_J > 1$. In some cases this choice of κ leads to an impractically large number of Monte Carlo steps required for the equilibration of the lattice gas and for the determination of the desired surface diffusion coefficients. Especially at very low temperatures and in ordered regions of the relevant phase diagram, hop events occur very infrequently. Therefore, smaller normalization factors $\kappa < \kappa_{max}$ can be chosen. However, it should be verified very carefully that in such cases the fraction of jumps with jump probabilities $P_J > 1$ is still negligibly small (<0.1%).

It is certainly important to note that eqns. (6) and (7) represent a mathematical recipe (or, in other words, a transition algorithm (TA)) describing how adatoms travel over a surface and how new system configurations evolve from preceeding ones. Different TA's are conceivable and have been used in the literature, some of them will be described in Section 4.

The procedure for simulating jumps in the canonical ensemble has been described in some detail in refs. 14 and 28 and, therefore, we will present only the general schema of the computations. First, for a given lattice gas configuration an initial site i is randomly picked. If filled, an adjacent final site j is randomly selected. If the destination is vacant, a jump may occur with probability P_J (eqn. (7)), otherwise, no jump occurs. Thermodynamic equilibrium is established before starting a diffusion run at the desired fixed coverage θ. Approach to equilibrium is monitored by following the configurational energy and in case of ordering by measuring corresponding order parameters of the system. Equilibrium is assumed to be established when these quantities fluctuate about their average values. In a recent publication, we have shown that in some systems even minute deviations from thermodynamic equilibrium may substantially influence the surface diffusion coefficients.[29]

In the MC method the tracer diffusion coefficient D_t can be easily determined from measurements of the mean square displacements of N tagged adatoms according to eqn. (1). The displacements $\Delta r_i(t)$ are expressed in units of the lattice constant a_0.

3 Finite-size scaling of surface diffusion coefficients

In a recent Monte Carlo study, the finite-size scaling concept has been extended to kinetic and dynamic quantities. In ref. 30 we have investigated the tracer diffusion coefficient D_t of interacting particles in the vicinity of a second order surface phase transition. The system studied was the square lattice gas with nearest neighbor repulsive interactions, φ_{NN}. Its interaction dependent part of the Hamiltonian is given by

$$\mathcal{H} = -\varphi_{NN} \sum_{NN} c_i c_j. \quad (9)$$

Here the $c_{i,j} = 0,1$ denote local occupation variables for each discrete lattice site. This well-known and frequently studied system exhibits c(2 × 2) ordering below the critical temperature $T_c = 0.567 \varphi_{NN}/k_B$.[31–33] Probably the most striking result of ref. 30 was the observation that D_t depends on the lattice size L of the lattice near T_c. For all values of L studied, $D_t(T)_{\theta=0.5}$ is a smooth function and exhibits an inflexion point at or near T_c. Its derivative, $\partial D_t/\partial(1/k_B T)$, exhibits a cusp-like maximum which is sharply pronounced at least for larger values of L. The temperatures where these maxima occur converge to $T_c(\infty)$ for large L. In refs. 30 and 34 we have analysed the finite-size scaling behavior of the tracer diffusion coefficient using the scaling dependence,[35,36]

$$D_t = D_t^{crit} + \varepsilon^{\sigma_t} \tilde{D}_t(L^{1/\nu}\varepsilon) + \ldots \quad (10)$$

where $\sigma_t = 0.665 \pm 0.03$ and $\tilde{D}_t$ are the corresponding critical exponent and scaling function, respectively. ε represent the reduced temperature, $1 - T/T_c$, and ν is the critical exponent of the correlation length ξ. Note that the leading term (which remains present at $\varepsilon = 0$) is the regular part (without any singular behavior) of the corresponding diffusion coefficient. Taking the derivative of eqn. (10) yields

$$\frac{\partial D_t}{\partial(\varphi_{NN}/k_B T)} \propto \varepsilon^{\sigma_t - 1} \tilde{D}_t(L^{1/\nu}\varepsilon) \propto L^{\frac{1-\sigma_t}{\nu}} \tilde{D}_t(L^{1/\nu}\varepsilon). \quad (11)$$

Eqn. (11) is valid for $L \to \infty$, $\varepsilon \to 0$ and finite values of $L^{1/\nu}\varepsilon$. Consequently, the scaling behavior of the maximum of the derivative, eqn. (11), $|\partial D_t/\partial(\varphi_{NN}/k_B T)|_{max}$, should be given by

$$\left| \frac{\partial D_t}{\partial(\varphi_{NN}/k_B T)} \right|_{max} \propto L^{\frac{1-\sigma_t}{\nu}}. \quad (12)$$

4 Does the critical exponent σ_t depend on the TA?

In this paper we address the important question if the critical exponent σ_t depends on the transition algorithm (TA). In order to motivate this issue, we recall that the occupation numbers, c_i in eqn. (9), change in time due to adatom jumps. The statistical description of the dynamics of adatom migration is defined through the transition probability w_{if} describing an adatom jump from an initial site i with energy ε_i to a final site f with energy ε_f,

$$w_{if} = \nu_{ij} c_i (1 - c_j) \Delta t. \tag{13}$$

Here ν_{ij} is the jump frequency of the corresponding event $i \rightarrow j$ and Δt is the time interval of a single MC step. However, eqn. (13) does not determine transition probabilities unequivocally. In fact, different choices for the energy and temperature dependences of ν_{ij} have been used in the literature according to the underlying microscopic model in the description of adatom jumps. The first one was inroduced by Metropolis in 1953[37]

$$\nu_{if}^{MP} = \min\left\{\nu, \nu \exp\left(\frac{\varepsilon_i - \varepsilon_f}{k_B T}\right)\right\}. \tag{14}$$

The MP algorithm favors those jumps which decrease the free energy of the system. Thus, the system reaches thermodynamic equilibruim in a lesser number of MC steps (MCS). A rather similar form for the transition probability was supposed by Kawasaki,[38–40]

$$\nu_{if}^{KS} = \nu\left[1 + \exp\left(\frac{\varepsilon_f - \varepsilon_i}{k_B T}\right)\right]^{-1}. \tag{15}$$

Eqn. (15) differs from the Metropolis form only in a narrow energy interval $|\varepsilon_i - \varepsilon_f| \leq k_B T$.

Another form of the jump frequency was introduced in ref. 41 taking into account the particular situation encountered in the case of surface diffusion of classical heavy particles which do not tunnel through the potential barrier. In such a situation, the main factor determining the probability of jump, is whether the adatom has an energy large enough to overcome the potential barrier ΔE. This quantity in a first approximation can be written as the difference of the adatom energies at the saddle point (ε_{sp}) and in the initial potential minimum at site i, $\Delta E = \varepsilon_{sp} - \varepsilon_i$. The transition probabilities are then given by

$$\nu_{if} = \nu \exp\left(\frac{\varepsilon_i - \varepsilon_{sp}}{k_B T}\right). \tag{16}$$

However, in practice one frequently assumes ε_{sp} as a constant for all possible adatom jumps, *i.e.* the associated jump probabilities are given by[5]

$$\nu_{if}^{IV} = \nu \exp\left(\frac{\varepsilon_i}{k_B T}\right). \tag{17}$$

This simplification is the basis of the initial value (IV) transition algorithm being used in refs. 30 and 42. More realistic assumptions considering the influence of adatom interactions at the barrier have been considered for instance in refs. 43 and 44.

Neither the MP nor the KS algorithms do explicitly consider the influence of the energetic barrier between initial and final sites. The transition dynamics (TD) algorithm[45] is similar to the MP algorithm, but uses an adjustable parameter Δ to account for the diffusion barrier.

It is quite obvious that the transition algorithms discussed so far can be subdivided in two classes, those which depend on the energy of the final state ε_f (MP, KS and TD) and others which do not (IV). It should be noted that ν in eqns. (14)–(17) is a normalization constant.

5 Results and discussion

In this work we investigate the finite-size scaling behavior of the tracer surface diffusion coefficient, D_t, using the IV, MP and KS transition algorithms. For this purpose we applied the MC algorithm, which is described in detail in refs. 9, 14, 29, 46 and 47. In the present work a fully parallelized version of our algorithm was run either on the Cray T3E (LC672-128) operated by the Max-Planck community in Garching/Germany or on the Rutgers Beowulf cluster consisting of 70 low-cost LINUX PC's.

The temperature dependences of the tracer diffusion coefficients D_t (calculated directly *via* eqn. (1)), are presented in Fig. 1. As in previous studies,[19,14] the calculated diffusion coefficients are normalized with respect to D^o, the chemical diffusion coefficient of the non-interacting Langmuir gas. It is important to note, that the diffusion data shown represent true thermodynamic equilibrium at given values of temperature T and lattice size L. In Fig. 1 we focus on a relatively narrow range of temperatures around T_c.[49] Obviously, the general shape of the D_t *vs.* $1/T$ graphs is rather similar for all TA's investigated. However, the absolute values of D_t/D^o differ con-

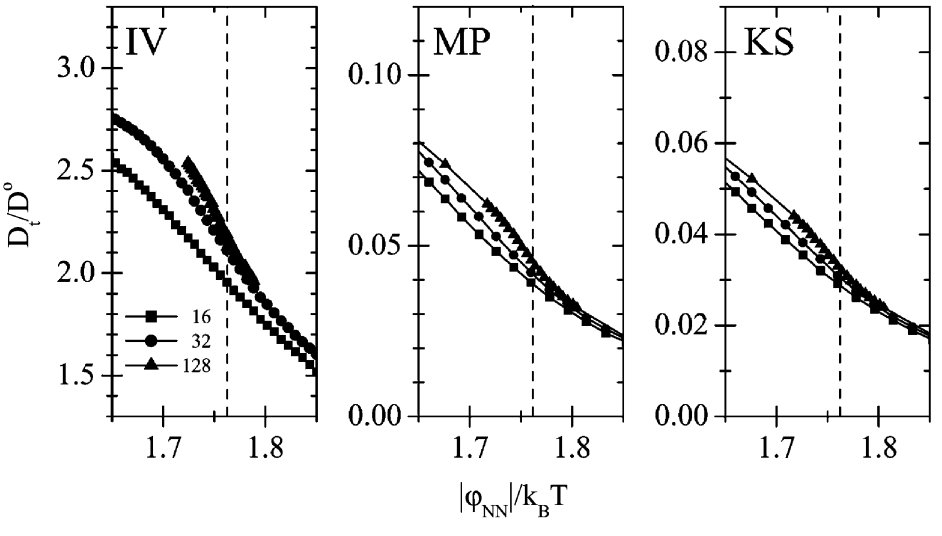

Fig. 1 Normalized tracer surface diffusion coefficient, D_t/D^o, *vs.* $\varphi_{NN}/k_B T$. As in previous studies,[14,48] the tracer diffusion coefficient is normalized with respect to D^o, the chemical diffusion coefficient of the Langmuir gas. Results are shown for the IV, MP and KS dynamics. The calculations are performed at half coverage, $\theta = 0.5$, for various lattice sizes L as indicated. The dotted line corresponds to $\varphi_{NN}/k_B T_c = 1.76$.

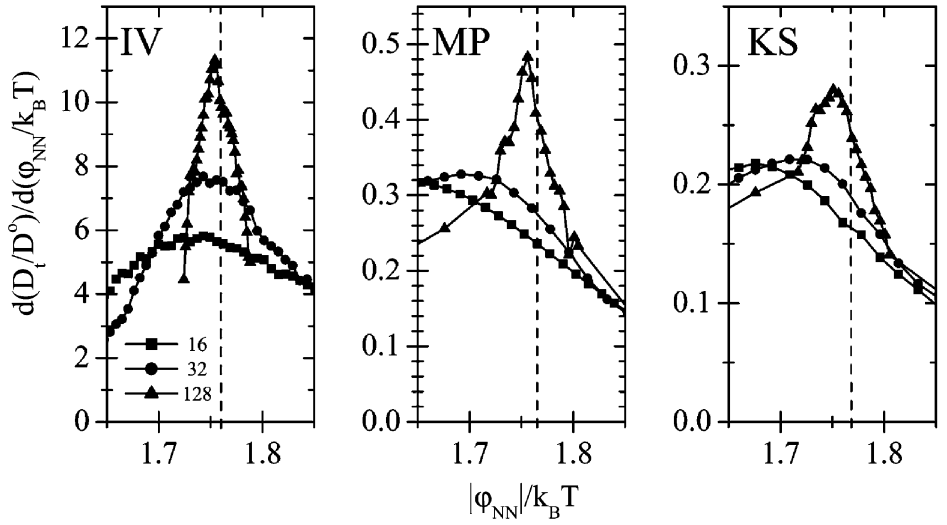

Fig. 2 Derivative of the normalized tracer diffusion coefficient with respect to $|\varphi_{NN}/k_BT|$. Results are shown for the IV, MP and KS dynamics. The calculations are performed at half coverage, $\theta = 0.5$, for various lattice sizes L as indicated. The vertical line corresponds to $\varphi_{NN}/k_BT_c = 1.76$.

siderably. The IV TA yields $D_t/D^o > 1$, *i.e.* tracer diffusion is accelerated relative to the noninteracting case, while KS and MP TA's indicate the opposite. This striking finding can be explained by the underlying atomistic picture. The IV algorithm assumes the probability of each jump to depend on the initial site energy (eqn. (17)). Therefore, at finite coverage repulsive NN interactions accelerate all jumps, and this causes $D_t^{IV}/D^o > 1$. In contrast, for the MP and KS algorithms the jump probabilities depend on $\varepsilon_f - \varepsilon_i$, *i.e.* only jumps from highly coordinated to less coordinated lattice sites are accelareted by the NN repulsions, all other jumps are decelerated. The net effect for both algorithms is negative, *i.e.* $D_t^{KS,MP}/D^o < 1$. The most striking finding of Fig. 1 is clearly the significant lattice size dependences of D_t near T_c. For a given temperature close to T_c, the values of D_t increase with increasing L.

Fig. 1 also shows that, regardless of the TA considered, there are weak turning points near T_c, which are clearly seen as maxima in the derivatives $|\partial D_t/\partial(\varphi_{NN}/k_BT)|$ (Fig. 2). The maxima are very wide for the small lattices, but are drastically sharpened upon increasing L. In order to describe the finite-size scaling behavior of D_t, we assume the scaling dependence of eqn. (10).[35,36] Our analysis shown in Fig. 3 yields $\sigma_t^{IV} = 0.66 \pm 0.02$, $\sigma_t^{MP} = 0.59 \pm 0.02$ and $\sigma_t^{KS} = 0.67 \pm 0.02$ for the different TA's. The critical exponents for the IV and KS TA's appear to be identical within statistical limts. However, the corresponding value for the MP TA is significantly off. Therefore, our results suggest that the critical approach to the thermodynamic limit depends to some extent on the underlying microscopic picture of adatom migration. In other words, the critical exponents of the tracer diffusion coefficient may present different values depending of the TA used to mimic adatom jumps on the surface.

Fig. 2 also shows another interesting feature. The position of the maxima, $K_c(L) \equiv \varphi_{NN}/k_BT_c(L)$, depends on lattice size L as well (Fig. 4). For the description of $K_c(L)$ we assume

$$K_c(L) = K_c(\infty) + AL^{-1/\nu}, \quad L \to \infty. \tag{18}$$

Here $K_c(\infty)$ is the critical temperature in the thermodynamic limit and A is a constant. The extrapolation of $K_c(L)$ for the IV and KS TA gives a critical temperature $K_c(\infty) = 1.76$ in good agreement with the theory, Fig. 4, while the corresponding value for the MP TA is $K_c(\infty) = 1.78$ is slightly higher. Nevertheless, it is obviously possible to use surface diffusion data to obtain critical temperatures using finite-size scaling arguments.

In order to explain the finite-size dependence of the tracer diffusion coefficient, we note that the tracer diffusion coefficient can be approximately expressed as a product of a tracer correlation factor f,[50,51] a vacancy availability factor V and an average jump probability $\langle P_J \rangle$,[15,52]

$$D^* = fV\langle P_J \rangle. \tag{19}$$

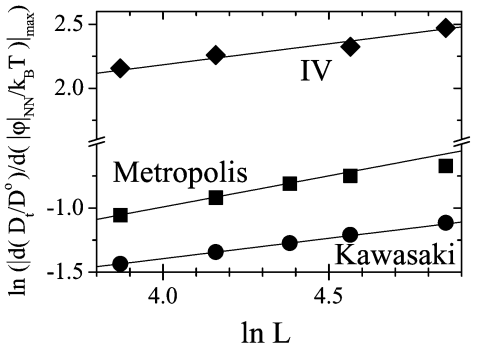

Fig. 3 Logarithm of the derivative of D_t *vs.* logarithm of the lattice size L. The values shown represent the maxima obtained from corresponding Arrhenius diagrams such as shown in Fig. 2. The solid lines are least square fits being used to obtain the slope $(1 - \sigma_t)/\nu$ and the corresponding critical exponent σ_t.

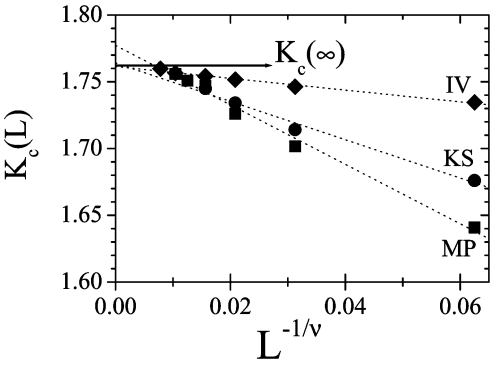

Fig. 4 Position of the maxima of the derivate of D_t/D^o as shown in Fig. 2. The temperature of the maxima is plotted in units of $K_c(L) \equiv \varphi_{NN}/k_BT_c(L)$ *vs.* $L^{-1/\nu}$.

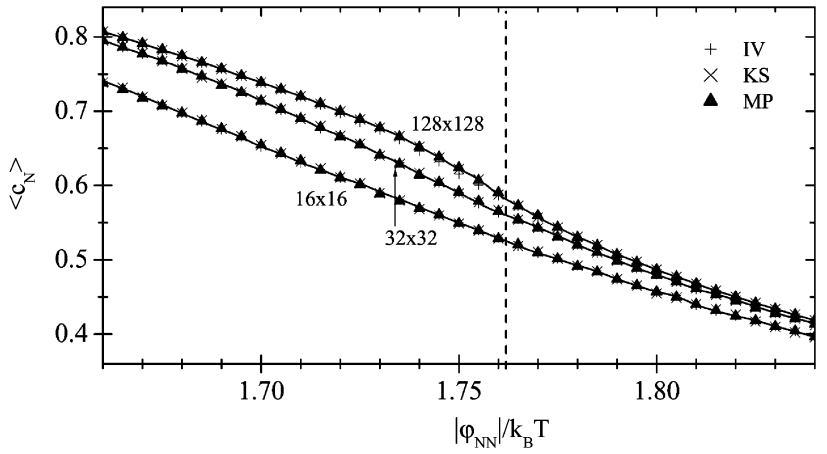

Fig. 5 Average coordination number, $\langle c_N \rangle$ for the IV, MP and KS dynamics. The calculations are performed at half coverage, $\theta = 0.5$, for various lattice sizes L as indicated. The vertical line corresponds to $\varphi_{NN}/k_BT_c = 1.76$. Note that $\langle c_N \rangle = 4(1 - V)$.

It is interesting to realize that V is a purely thermodynamic quantity, which should not depend on the TA. In Fig. 5 we show the average coordination number, $\langle c_N \rangle = 4(1-V)$, for the various TA's. $\langle c_N \rangle$ exhibits a significant lattice size dependence but, as expected, is independent of the TA chosen. Therefore, this quantity does not account for the different finite-size scaling of D_t for the different TA's. $\langle c_N \rangle$ is proportional to the coordination energy of the lattice gas system. Its finite-size dependence, therefore, points to the scaling behavior of the specific heat, given by

$$C = \left(\frac{\varphi_{NN}}{k_B T}\right)^2 \theta L^2 (\langle c_N^2 \rangle - \langle c_N \rangle^2). \qquad (20)$$

The behavior of this static quantity, which is shown in Fig. 6, exhibits similarities with the derivate of D_t shown in Fig. 2. There are tiny and wide maxima for small lattice sizes L, which are sharpening and increasing as L is increased. However, the measured values of the specific heat do not depend on the TA, in contrast to the intriguing behavior of D_t and its derivative. In principle, Fig. 6 could be used to investigate the finite-size scaling behavior of the specific heat, as well. However, this has been done already a long time ago and is certainly not on the agenda of this paper. Nevertheless, Figs. 6 and 7 clearly show that static/thermodynamic and kinetic/dynamic quantities may exhibit different behavior with respect to finite-size scaling.

In ref. 30 we have argued that the finite-size dependency of the tracer diffusion coefficient is largely due to the behavior of the $\langle P_J \rangle$, which is different for the three TA's investigated here. This is shown in Fig. 7. First thing to note is that the absolute values $|P_J|$ are substantially different for the three TA's. However, it is also quite obvious that near criticality the variation of P_J with L is different for the various TA's.

6 Summary

In this work we have investigated the finite-size scaling behavior of the tracer surface diffusion coefficient, D_t, using the IV, MP and KS transition algorithms. However, one should have in mind that these TA's represent different mathematical recipes how new system configurations evolve from preceeding ones. Each TA favors a different physical picture of adatom jumps on a model surface.

We conclude that the finite-size scaling treatment of D_t near a second order phase transition can be done using the general scheme presented in ref. 30 regardless of the TA used to mimic microscopic jumps of adatoms. However, a different diver-

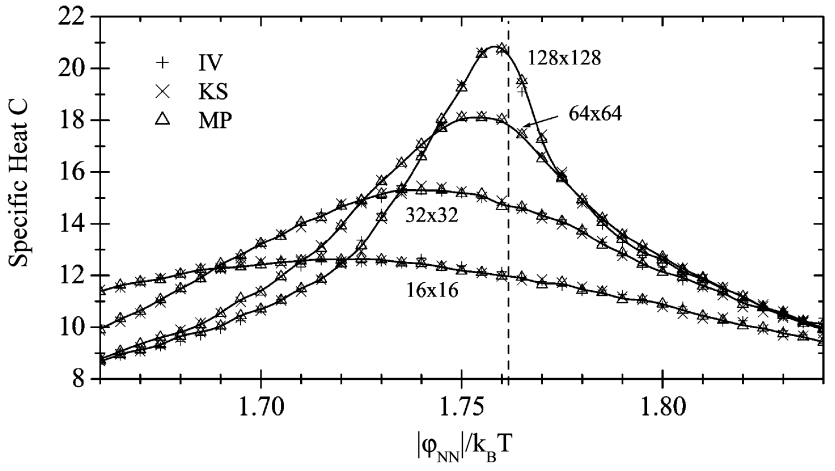

Fig. 6 Specific heat obtained according to eqn. (20) for the IV, MP and KS dynamics. The calculations are performed at half coverage, $\theta = 0.5$ for various lattice sizes L as indicated. The vertical line corresponds to $\varphi_{NN}/k_BT_c = 1.76$.

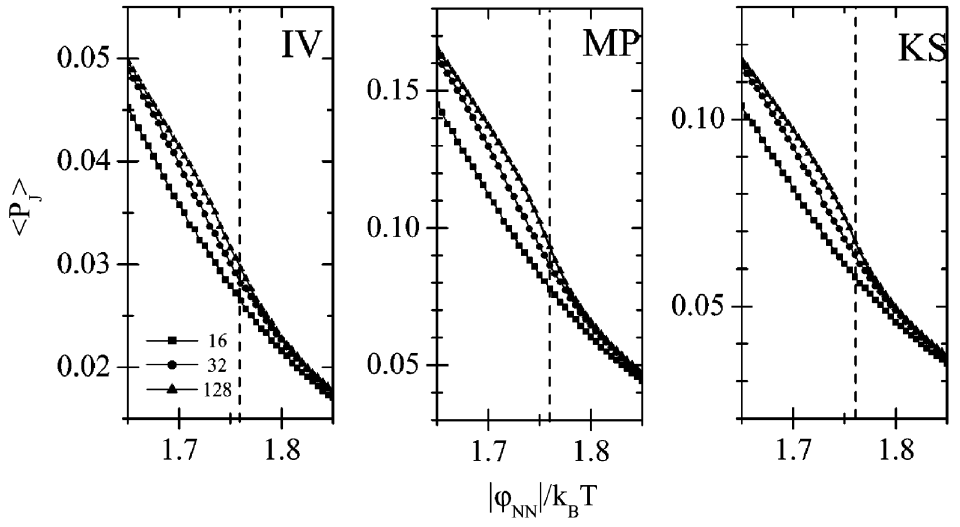

Fig. 7 Average jump probability, $\langle P_J \rangle$, for the IV, MP and KS dynamics. The calculations are performed at half coverage, $\theta = 0.5$, for various lattice sizes L as indicated. The vertical line corresponds to $\varphi_{NN}/k_B T_c = 1.76$.

gence of $|\partial D_t/\partial(\varphi_{NN}/k_B T)|$ towards the thermodynamic limit is observed according to the TA used. In fact, the critical exponent associated with the tracer diffusion coefficient, σ_t, exhibits characteristic values ($\sigma_t^{IV} = 0.66 \pm 0.02$, $\sigma_t^{MP} = 0.59 \pm 0.02$, $\sigma_t^{KS} = 0.67 \pm 0.02$), which are identical for the IV and KS TA's within error limits but significantly differ for the MP TA. Therefore, the results presented here suggest that the critical properties of the tracer diffusion coefficient are influenced by the choice of the transition algorithm. We hope to investigate different transport/diffusion coefficients and dynamic properties in order to generalize this idea in the future.

Acknowledgement

This work has been supported by the Heisenberg program of the Deutsche Forschungsgemeinschaft (DFG), by the Fonds der chemischen Industrie (FCI), by CONICET (Argentina) and by the National Agency for Promotion of Science and Technology (APCyT, Argentina), Proy. PICT98 N° C-03-03232. The authors would like to thank R. Gomer, V. Pereyra, G. Zgrablich and V. P. Zhdanov for encouraging and stimulating discussions.

References

1 A. Danani, R. Ferrando, E. Scalas and M. Torri, *Surf. Sci.*, 1998, **402**, 281.
2 T. Ala-Nissila and S. C. Ying, *Phys. Rev. B*, 1990, **42**, 10 264.
3 A. A. Tarasenko and A. A. Chumak, *Fiz. Tverd. Tela (Leningrad)*, 1982, **24**, 2972; A. A. Tarasenko and A. A. Chumak, *Sov. Phys. Solid State*, 1982, **24**, 1683.
4 Z. W. Gortel, M. A. Zoluska-Kotur and L. A. Turski, *Phys. Rev. B*, 1995, **52**, 16916.
5 A. A. Chumak and A. A. Tarasenko, *Surf. Sci.*, 1980, **91**, 694.
6 A. A. Tarasenko and A. A. Chumak, *Poverkhnost (in Russian)*, 1989, **11**, 98.
7 A. A. Tarasenko, L. Jastrabik and C. Uebing, *Phys. Rev. B*, 1998, **57**.
8 A. A. Tarasenko, L. Jastrabik, F. Nieto and C. Ubing, *Phys. Rev. B*, 1999, **59**, 8252.
9 A. V. Myshlyavtsev, A. A. Stepanov, C. Uebing and V. P. Zhdanov, *Phys. Rev. B*, 1995, **52**, 5977.
10 J. W. Haus and K. W. Kehr, *Phys. Rep.*, 1987, **150**, 263.
11 T. Ala-Nissila, W. K. Han and S. C. Ying, *Phys. Rev. Lett.*, 1992, **68**, 1866.
12 I. Vattulainen, J. Merikoski, T. Ala-Nissila and S.C. Ying, *Phys. Rev. Lett.*, 1997, **79**, 257.
13 M. A. Zoluska-Kotur and L.A. Turski, *Phys. Rev. B*, 1994, **50**, 16 102.
14 C. Uebing and R. Gomer, *J. Chem. Phys.*, 1991, **95**, 7626; C. Uebing and R. Gomer, *J. Chem. Phys.*, 1991, **95**, 7636; C. Uebing and R. Gomer, *J. Chem. Phys.*, 1991, **95**, 7641; C. Uebing and R. Gomer, *J. Chem. Phys.*, 1991, **95**, 7648.
15 K. Kehr and K. Binder, in *Applications of the Monte Carlo Method in Statistical Physics*, of *Topics in Current Physics*, ed. K. Binder, Springer-Verlag, Berlin, 2nd edn., 1987, vol. 36, p. 181.
16 K. Binder, in *Phase Transitions and Critical Phenomena*, ed. C. Domb and J. L. Lebowitz, Academic Press, New York, 1983, vol. IIX, p. 1.
17 E. Bauer, in *Structure and Dynamics of Surfaces II*, ed. W. Schommers and P. von Blanckenhagen, Springer, Berlin, 1987, p. 115.
18 S. K. Ma, *Modern Theory of Critical Phenomena*, Benjamin, Reading, MA, 1976.
19 D. P. Landau, in *Monte Carlo Methods in Statistical Physics*, ed. K. Binder, Springer-Verlag, Berlin, 1979.
20 D. P. Landau, in *Applications of the Monte Carlo Method*, ed. K. Binder, Springer-Verlag, Berlin, 1987.
21 K. Binder and D. P. Landau, *Surf. Sci.*, 1976, **61**, 577.
22 K. Binder and D. P. Landau, *Phys. Rev.*, 1980, **B 21**, 1941.
23 R. Gomer, *Rep. Prog. Phys.*, 1990, **53**, 917.
24 G. D. Billing and K. V. Mikkelsen, in *Introduction to Molecular Dynamics and Chemical Kinetics*, Wiley-Interscience, 1996.
25 D. C. Rapaport, in *The Art of Molecular Dynamics Simulation*, Cambridge, 1997.
26 J. M. Haile, in *Molecular Dynamics Simulation: Elementary Methods*, Wiley-Interscience, 1997.
27 M. Tringides and R. Gomer, *Surf. Sci.*, 1986, **166**, 419.
28 M. Tringides and R. Gomer, *Surf. Sci.*, 1984, **145**, 121.
29 C. Uebing and R. Gomer, *J. Chem. Phys.*, 1994, **100**, 7759.
30 F. Nieto, A. A. Tarasenko, and C. Uebing, *Europhys. Lett.*, 1998, **43**, 558.
31 L. Onsager, *Phys. Rev.*, 1944, **65**, 117.
32 C.N. Yang, *Phys. Rev.*, 1942, **85**, 808.
33 B. M. McCoy and T. T. Wu, *The two-dimensional Ising model*, Harvard University, Cambridge, MA, 1977.
34 F. Nieto and C. Uebing, *Ber. Bunsen-Ges. Phys. Chem.*, 1998, **102**, 974.
35 K. Binder, in *Finite Size Scaling and Numerical Simulation of Statistical Systems*, ed. V. Privman World Scientific, Singapore, 1990.
36 K. Binder, *Rep. Prog. Phys.*, 1997, **60**, 488.
37 N. Metropolis *et al.*, *J. Chem. Phys.*, 1953, **21**, 1087.
38 K. Kawasaki, *Phys. Rev.*, 1966, **145**, 224.
39 K. Kawasaki, *Phys. Rev.*, 1966, **148**, 375.
40 K. Kawasaki, *Phys. Rev.*, 1966, **150**, 285.
41 C. Uebing and V. P. Zhdanov, *J. Chem. Phys.*, 1998, **109**, 3197.
42 C. Elke Clauberg, C. Uebing, H. Viefhaus, and H. J. Grabke, in *Proceedings of the 9th International Conference on Intergranular and Interphase Boundaries in Materials (iib)*, ed. Pavel Lejcek

and Vclav Paidar, Trans Tech Publications, 1999, vol. 294–296, p. 465.
43 C. Uebing and R. Gomer, *Ber. Bunsen-Ges. Phys. Chem.*, 1996, **100**, 1138.
44 C. Uebing and R. Gomer, *Surf. Sci.*, 1997, **381**, 33.
45 T. Ala-Nissila, J. Kjoll, and S. C. Ying, *Phys. Rev.*, 1992, **B 46**, 846.
46 C. Uebing, *Phys. Rev. B*, 1994, **49**, 13 913.
47 C. Uebing and R. Gomer, *Surf. Sci.*, 1995, **331–333**, 930.
48 E. C. Viljoen and C. Uebing, *Langmuir*, 1997, **13**, 1001.
49 For a discussion of the general temperature dependence of D_t and D_j over a much wider range of temperatures, see ref. 14.
50 A. D. LeClaire, in *Physical Chemistry—An Advanced Treatise*, ed. H. Eyring, D. Henderson and W. Jost, Academic Press, New York, 1970, vol. 10.
51 G. E. Murch, *Philos. Mag.*, 1981, **A 43**, 871.
52 G. E. Murch and R. J. Thorn, *J. Phys. Chem. Solids*, 1977, **38**, 789.